This article has been accepted for publication in a future issue of this journal, but has not been fully edited. Content may change prior to final publication. Citation information: DOI 10.1109/ACCESS.2018.2828878, IEEE Access

Characteristic Mode Design of Wide Band Circularly Polarized Patch Antenna Consisting of H-Shaped Unit Cells

Chen Zhao, *member*, *IEEE*, Chao-Fu Wang, *Senior Member*, *IEEE*

***Abstract*—This paper proposes a general characteristic mode (CM) based design procedure of simple three steps for wideband circularly polarized (CP) antenna design. First of all, the characteristic mode analysis is carried out to understand the different modes of a proposed antenna geometry without feeding network. Secondly, modal currents and their corresponding modal fields (radiation patterns) are studied for choosing modes to shape the required radiation pattern. Finally, a suitable feeding structure is chosen to excite the desired modes at the same time owns a good impedance matching. As an example, a CP patch antenna fed with cross-shaped aperture is proposed and designed following the design procedure. Patch consisting of H-shaped unit cells are used as the radiator. Characteristic mode method is applied to analyze the modes of the proposed antenna and explains the property of wide band circular polarization. It is revealed that higher order modes of the patch can be used to achieve circular polarization over a wideband of frequency. The antenna is fabricated using printed circuit techniques. The return loss and radiation properties are measured and compared with simulation results. With the highly coupled units, a wide impedance bandwidth of 38.8% is obtained. Besides, a wide 3-dB axial ratio bandwidth of 14.3% is achieved.**

***Index Terms*— characteristic mode theory, circular polarization, wide band**

I. INTRODUCTION

WIRELESS communication requires circularly polarized (CP) antennas with wide bandwidth, high gain and low profile. Microstrip antenna is a good candidate as it owns the advantages of low profile and easy fabrication. CP microstrip patch antenna can be achieved with single-feed or multi-feed techniques [1], [2]. Truncated square patch antenna, slotted patch antenna are popular CP patch antennas. Rectangular patch with cross-shaped aperture feed has also been proposed to achieve the circular polarization [3].

Manuscript received September, 2017.
Zhao Chen is with the Nanjing University of Information and Technology, 219 Ning Liu Avenue, 210044. (e-mail: 002912@nuist.edu.cn)
Chao-Fu Wang is with Temasek Laboratories, National University of Singapore, 5A Engineering Drive 1, #09-02, Singapore 117411, Singapore (e-mail: cfwang@nus.edu.sg).
Color versions of one or more of the figures in this paper are available online at http://ieeexplore.ieee.org.

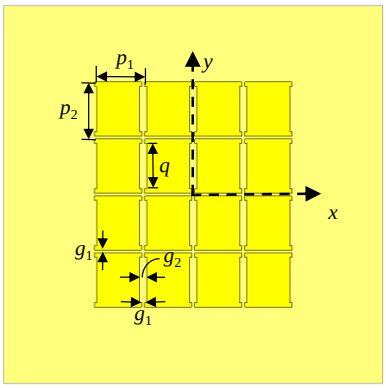

Fig. 1. Top view of the proposed antenna without feeding.

These antennas have low profile and can be easily fabricated. However, the limited bandwidth, especially the 3 dB axial ratio bandwidth, has always been the drawback of such antennas. The reason is that the two orthogonal modes own a same magnitude and 90-degree phase difference at only one single frequency. Generally, the bandwidth of patch antennas can be improved by using substrate with lower dielectric constant and higher thickness. Air substrate, for example, can improve the bandwidth a lot. But it makes the antenna quite thick and bulky, and cannot be easily fabricated using printed circuit technique. Another way of improving the bandwidth is to use double-feed CP antenna. It is achieved by feeding the antenna at two different feeding point with 90-degree phase difference in two orthogonal directions. The bandwidth of a cross-aperture coupled patch antenna can also be enhanced by using broadband couplers [4], [5]. But these CP antennas often involve complex feeding structures.

The mushroom-like metamaterial structures have been used to enhance the performance of antennas. It has been used as artificial magnetic conductor (AMC) or high impedance surface (HIS) to increase the bandwidth of low profile antennas [6]–[8]. A rectangular shaped HIS has also been used as ground to form the circular polarization and to increase the bandwidth of the 3-dB axial ratio [9], [10]. Recent studies have used square metamaterial patches as the patch radiator. It is able to provide a wider bandwidth for a linear polarized antenna from additional modes [11], [12]. From this point, a wide circular polarization bandwidth should be able to be achieved if the antenna can provide additional orthogonal modes with 90-degree phase difference.

TABLE I
DIMENSIONS OF THE PROPOSED ANTENNA IN MM

p_1	p_2	g_1	g_2	q
9.9	11.3	0.6	1.4	9

Characteristic mode (CM) theory developed in [13], [14] has been proved useful in antenna designs [15]. It gives a clear understanding of each resonant mode, the corresponding mode current, as well as its far field radiation pattern. This information can provide important guidance to design an antenna with maximized performance through finding the best feeding point, reducing antenna size and enhancing the bandwidth etc [15]–[25]. Recently, the CM theory has been used to analyze a metasurface based antenna with linear polarization [26]. But only the fundamental modes are used and the phase information of each mode is not studied which is actually quite useful for CP antenna design. Also, as the CM theory is independent of feeding structure, it can be used to have a "pre-check" on the radiation properties without the feeding, especially when the radiator has a complex shape.

In this paper, 4×4 H-shaped HIS unit cells are used as the radiator to form the patch antenna. The antenna is fed with a cross-shaped aperture. By analyzing the structure using CM theory [14], [15], it is found that such a patch antenna is able to achieve a wide CP bandwidth with proper modes. The current and radiation pattern of all the possible modes are analyzed. It is revealed that with selected characteristic modes, a constant phase differences in two orthogonal directions can be excited. The cross-shaped aperture is applied to feed the antenna which can be used to excite the required modes [27]. In addition, because of the extra capacitance brought by the patch with unit cells, the antenna is able to provide a good impedance matching over a very wide bandwidth.

This paper is organized as follows: In section II, the configuration of the antenna without feeding is proposed with detailed dimensions. Section III gives some reference equations for CM theory, after which the CM theory is used to analyze the existing modes in the antenna. Mode current and mode radiation pattern are studied to find the required modes. In Section IV, cross shaped aperture is chosen to excite the required modes with good impedance matching. The influence of the feeding structure to the *S* parameters and axial ratio is also studied. In Section V, a prototype of the proposed antenna is fabricated. Measured results are presented and compared with simulations. The paper ends with a conclusion in Section VI.

II. ANTENNA CONFIGURATION

The configuration of the antenna without feeding is presented in Fig. 1. As is shown, a 4×4 nonuniform 'H'-shaped patch array is printed on the top surface of the substrate. The substrate has a relative permittivity $\varepsilon_r = 3.38$ and thickness $h_1 = 3.048$ mm. The period of the unit is p_1 and p_2 in x and y directions, respectively. The gap between each unit is g_1 in both x and y directions. Here we start with H-shaped unit cell as it gives better circular polarization compared with a rectangular-shaped unit cell. With 4×4 unit cells, the antenna owns the potential to operate over wider frequency band. At the fundamental mode, the current flows on the whole antenna, contributing to radiation at lower frequencies. On the other hand, at higher modes, the mode current mainly flows on parts of the antenna (the inner 2×2 unit cells, for example), contributing to radiation at higher frequencies.

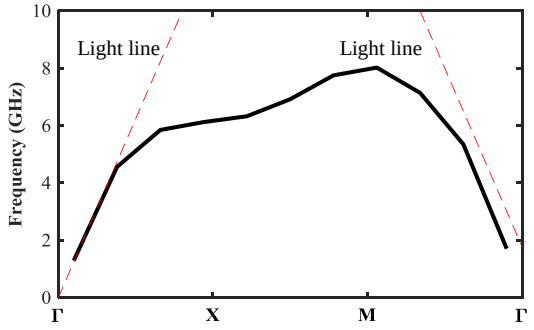

Fig. 2. Dispersion diagram over the Brillouin zone.

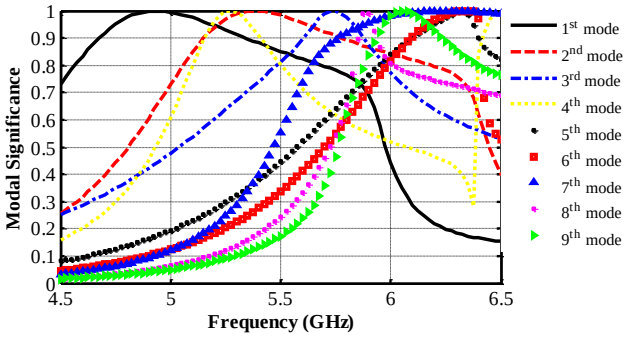

Fig. 3. Modal significance of the first 9 modes from 4.5 to 6.5 GHz.

The dimensions of the patch are presented in Table I. Unlike the normal patch antenna, the radiation happens not only at the edge but also at the slots between the units. That provides flexibility to change the phase of the far field electric field as more radiating modes are involved.

Fig. 2 shows the dispersion diagram (fundamental mode) of the H-shaped unit cell over the Brillouin zone. The two red dashed lines presents the dispersion diagram of light in the substrate. As is shown, the operating frequency of such unit cell changes from 4.5 GHz to about 8 GHz as phase changes. The phase velocity is slower than the speed of light in the substrate. That will lead to a more compact size of the antenna compared with square patch antenna.

III. CHARACTERISTIC MODE ANALYSIS

With nonuniform shape of the metalmaterial unit, the modes exited in these x and y directions differ with each other. With specific design, it is able to excite modes that have a phase difference of 90 degrees in two directions over a wide frequency range. With slots between unit cells, more than one mode can be excited. In order to have a better understanding of

This article has been accepted for publication in a future issue of this journal, but has not been fully edited. Content may change prior to final publication. Citation information: DOI 10.1109/ACCESS.2018.2828878, IEEE Access

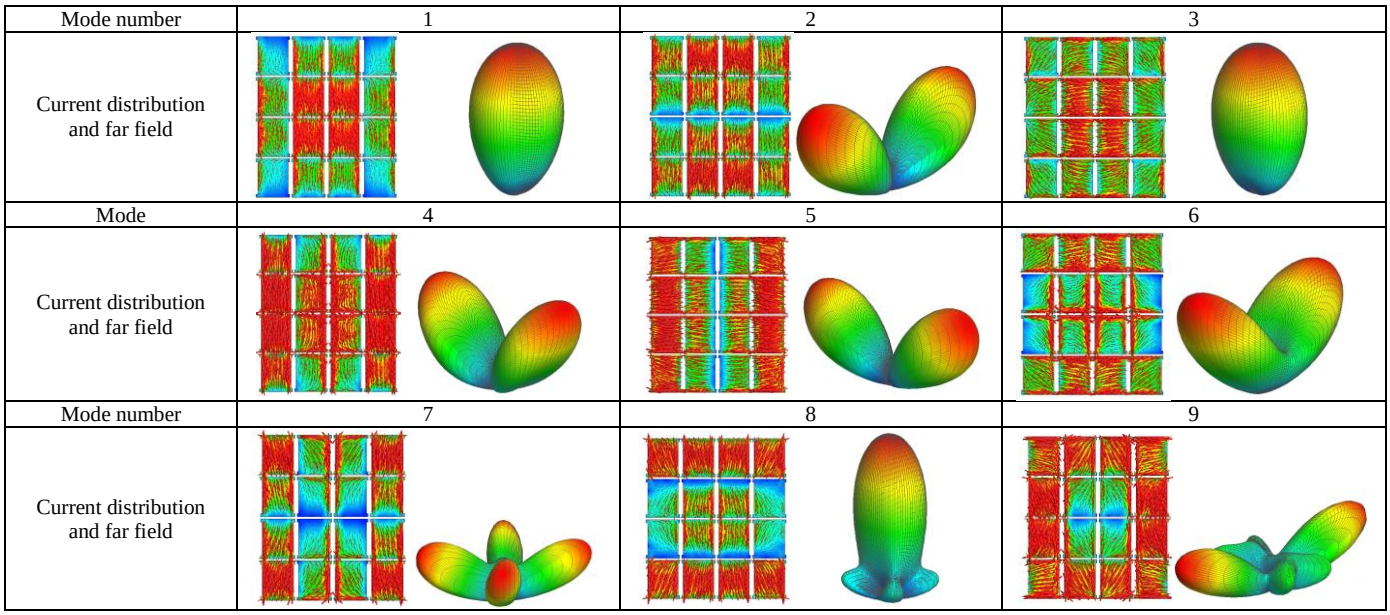

Fig. 4. Modal current distribution and modal field (far field radiation pattern) of 9 modes at 5.3 GHz.

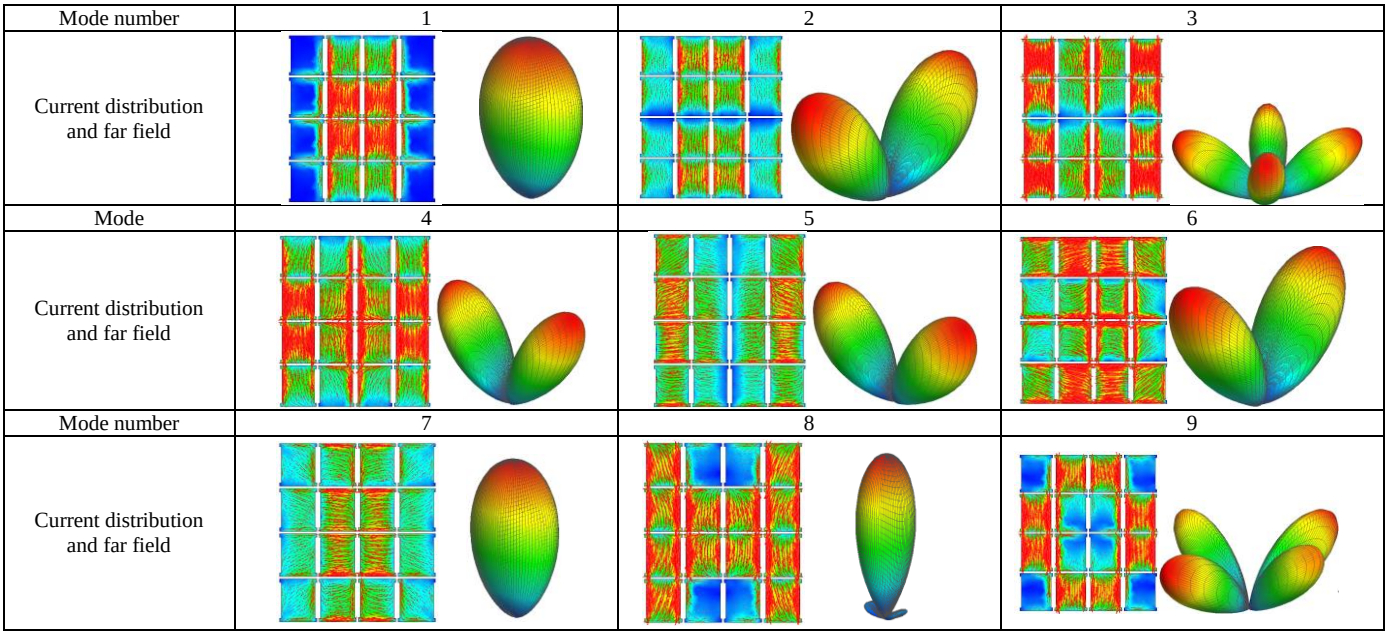

Fig. 5. Modal current distribution and modal field (far field radiation pattern) of 9 modes at 5.8 GHz.

the existing modes in the antenna, CM theory can be used to analyze this antenna. For ease of reference, some equations of CM theory are briefly presented here.

A. *Characteristic Mode Theory*

Two parameters namely the modal significance MS [16] and mode angle α [17] are obtained with the eigen value λ. These two parameters are independent of the excitation or source. The total current on the perfectly electrically conducting (PEC) body $\vec{J}$ can be expressed as the combination of different mode current:

$$\vec{J} = \sum_{n=1}^{N} c_n \vec{J}_n \tag{1}$$

where $\vec{J}_n$ is the mode current for mode n. c_n is the complex modal expansion coefficient which determines the weighing of each mode of the total current. Mode with a large $|c_n|$ means a dominate mode for the PEC body. On the other hand, $\vec{J}$ can also be expressed as [14]:

This article has been accepted for publication in a future issue of this journal, but has not been fully edited. Content may change prior to final publication. Citation information: DOI 10.1109/ACCESS.2018.2828878, IEEE Access

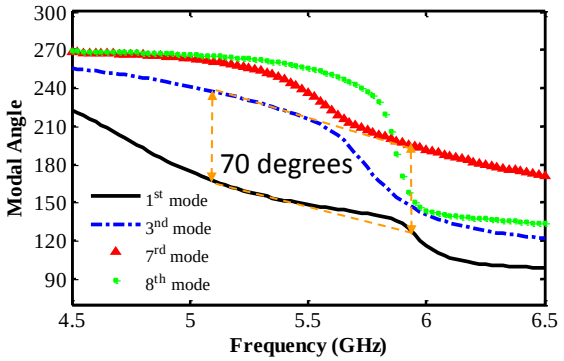

Fig. 6. Modal (characteristic) angle of mode 1, mode 3, mode 7 and mode 8.

$$\vec{J} = \sum_{n=1}^{N} \frac{V_n^i \vec{J}_n}{1 + j\lambda_n} \tag{2}$$

where V_n^i is called the modal excitation coefficient. From equation (1) and (2), we can get the expression for $|c_n|$:

$$|c_n| = \left|\frac{V_n}{1 + j\lambda_n}\right| = |V_n|MS \tag{3}$$

Equation (3) shows that there are two conditions to excite the desired mode. Not only a large modal significance is needed, but also a large modal excitation coefficient V_n is required. The modal excitation depends on the properties of feeding such as the feeding type, feeding position etc. So as to let an antenna to operate in a specific mode, it has to be fed properly. This method is not limited to all metal antennas and microstrip antennas, it can also be used for dielectric resonator antennas (DRA) with the development of CM theory for dielectric

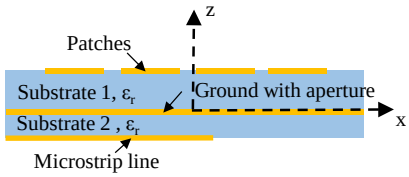

(a)

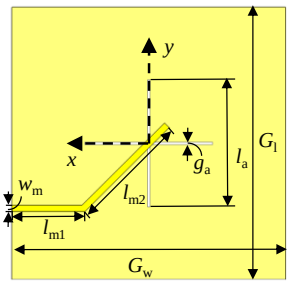

(b)

Fig. 7. (a) Side view of the feeding structure. (b) Top view of the feeding structure.

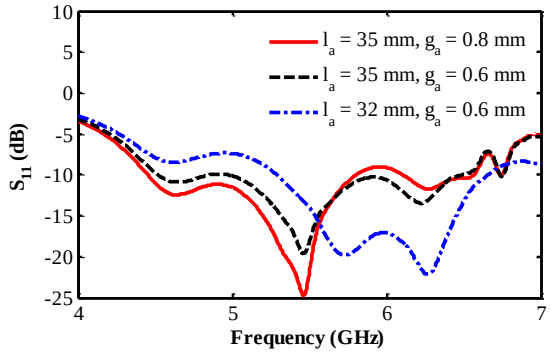

(a)

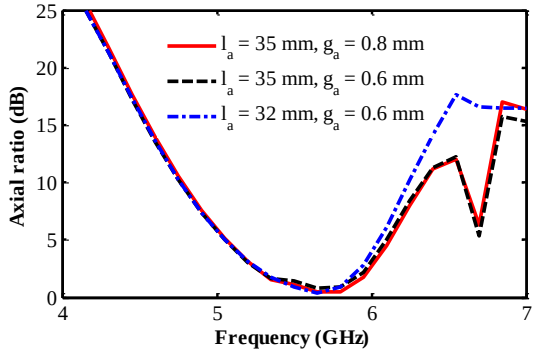

(b)

Fig. 8. (a) S_{11} and (b) axial ratio of the proposed antenna with different size of feeding aperture.

structures [28], [29]. In the following subsection, the modes of the proposed antenna are analyzed in details.

B. Existing Modes of the Proposed Antenna

In this paper, the antenna without feeding structure is analyzed using CM analysis. The substrate and the ground plane are considered infinite. The impedance matrix can be conveniently generated using FEKO after which an in-house Matlab CM theory code with robust mode tracking implementation [15] is used to carry out CM analysis from 4.5 to 6.5 GHz. Then, the calculated results are plotted by importing data back to FEKO. The modal significance of the first 9 modes is presented in Fig. 3. At lower frequencies, 4.5 GHz for example, only mode 1 has modal significance larger than 0.5 so that only mode 1 will dominate in the antenna. As frequency gets higher, more modes with relatively large modal significance are involved. In order to analyze the modes of the antenna clearly, the current and far field of different characteristic modes are studied. Fig. 4 presents the modal current and modal field (far field) of different modes at 5.3 GHz. We can see that among these modes, only mode 1, mode 3 and mode 8 radiate in the +*z* direction as the current on the patch is symmetric with respect to *xz* and *yz* planes. On the other hand, for the other modes (mode 2, mode 4, mode 5, mode 6, mode 7 and mode 9), the current is antisymmetric with respect to *xz* or *yz* planes. That will lead to a cancellation of electric field in the far field region in the +*z* direction (as is shown in Fig. 4). Besides, higher order modes (from mode 5 to mode 9) can

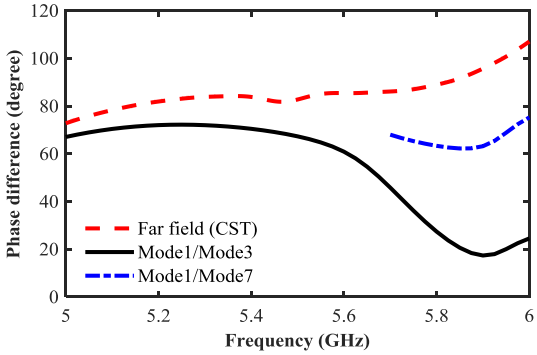

Fig. 9. Phase difference of far field and different modes in orthogonal directions.

TABLE II
DIMENSIONS OF THE FEEDING STRUCTURE IN MM

g_a	L_A	l_{m1}	l_{m2}	w_m	G_l	G_w
0.6	35	20	32.7	1.81	75	75

hardly be excited at this frequency as their modal significance is quite low. As a result, only mode 1 and mode 3 can be excited at 5.3 GHz. These two modes correspond to the fundamental mode in *y* and *x* directions, respectively. A circular polarization is formed when these two orthogonal modes have a phase difference of 90 degrees.

As frequency gets higher, some higher order modes are involved with modal significance higher than 0.5. The modal current and modal field (far field radiation pattern) of the first 9 modes at 5.8 GHz are presented in Fig. 5. Same with the lower frequency, mode 2, mode 3, mode 4, mode 5, mode 6 and mode 9 own antisymmetric mode current, resulting in a cancelation of field in +*z* direction. There are only 3 modes that are radiating in the +*z* direction. Mode 1 and mode 8 are the modes in the *y* direction. Mode 7 is the mode in *x* direction. Mode 1 is still dominant in the *y* direction until 5.8 GHz. Above 5.8 GHz, mode 8 and some other higher order mode will get in. It is noted that although the current for mode 8 is symmetric, the current on the outer two rows of units has a different direction with the inner two rows. That will lead to side lobe of the antenna at higher frequencies.

The phase of the required modes (radiating in +*z* direction) are presented in Fig. 6. It can be seen that unlike the traditional patch antenna. The phase difference between mode 1 and mode 3 is almost constant with a value of 70 degrees which is close to 90 degrees. As frequency goes above 5.5 GHz, the current of mode 3 becomes antisymmetric which cannot be excited. Instead, mode 7 is excited. If we look at the phase of mode 1 and mode 7, it can be seen that the phase difference between mode 1 and mode 7 is also around 70 degrees from 5.5 GHz to 5.8 GHz. However, when frequency goes up to 6 GHz. More modes will be involved which makes it difficult to analyze. The circular polarization performance will also become worse accordingly. A constant phase difference over the frequency band of interest ensures the potential of wideband CP. In addition, a well-designed feeding network can more or less

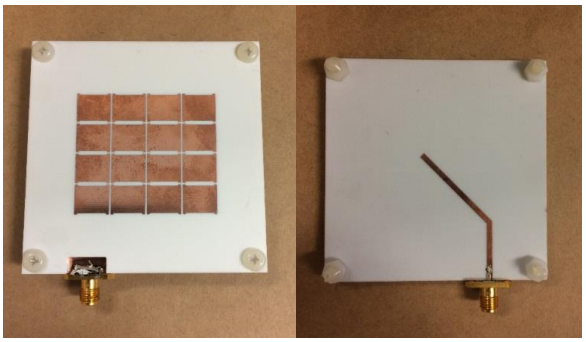

Fig. 10. Photos of the assembly.

contribute to certain phase difference as a compensation to the modal phase. This can be well explained by equation (2): when V_i is a complex value, the phase of the mode current can be varied.

IV. ANTENNA FEEDING NETWORK

A. Cross Aperture Feed

Knowing that only some of the modes are useful to us, it is necessary to feed the antenna properly so that the desired modes are excited while the undesired modes are not. In order to have a high gain at bore sight direction, the feeding should provide a good impedance matching for the symmetric mode without excitation of antisymmetric mode.

Usually there can be more than one type of feedings suitable for the antenna if there is only one mode with high modal significance. For example, probe feed, microstrip feed, and aperture feed, all can be used for rectangular patch antenna. When there are multiple modes at the frequency of operation, the feeding needs to excite the required mode without exciting other modes. This requirement gives more restrictions to the feed design. For the antenna proposed in this paper, symmetric current needs to be excited in case unrequired modes are excited. Besides, the ground plane should remain same with the model for CM analysis as much as possible in order to keep the CM results with less perturbation. Considering these factors, aperture feed is a good choice for the antenna.

Aperture feed can provide a large electric coupling at where the aperture is. From Figs. 4 and 5, we can see the

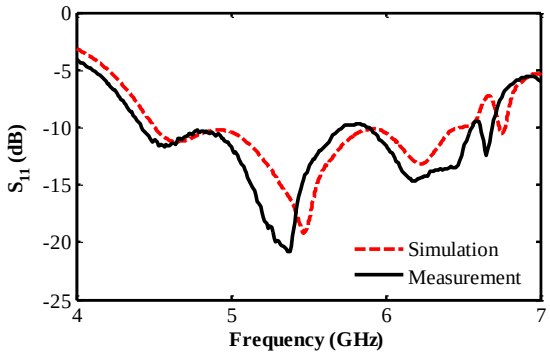

Fig. 11. Simulated and measured S parameter.

This article has been accepted for publication in a future issue of this journal, but has not been fully edited. Content may change prior to final publication. Citation information: DOI 10.1109/ACCESS.2018.2828878, IEEE Access

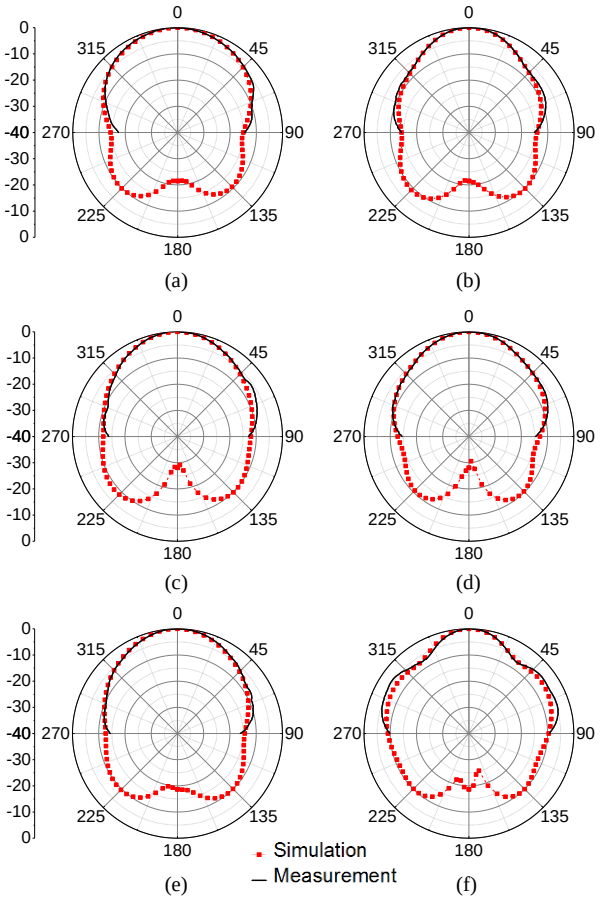

Fig. 12. Measured and simulated radiation pattern of the proposed antenna: (a) *xz*-plane at 5.2 GHz. (b) *yz*-plane at 5.2 GHz. (c) *xz*-plane at 5.5 GHz. (d) *yz*-plane at 5.5 GHz. (e) *xz*-plane at 5.8 GHz. (f) *yz*-plane at 5.8 GHz.

current/magnetic field of mode 1, mode 3 and mode 7 is highest at the center gap. From the current distribution of the modes, the magnetic current of the aperture should be in same direction of the mode current and placed at where the current is maximum. Besides, when the aperture is positioned at the center, the two halves of the antenna are symmetric with respect to the aperture. That will lead to a symmetric current distribution with respect to the aperture. The modes with antisymmetric mode current can hardly be excited.

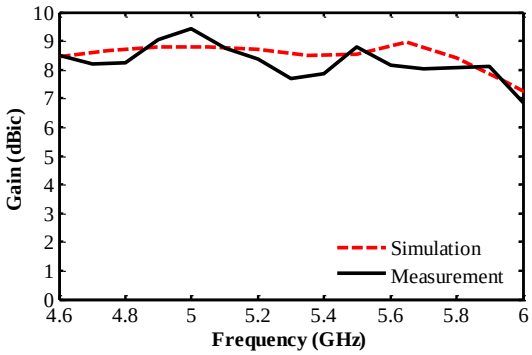

Fig. 13. Measured and simulated Gain at different frequencies.

The side view and top view of the cross-shaped aperture is shown in Fig. 7. The feeding structure is formed on an extra substrate. The substrate has a relative permittivity $\varepsilon_r = 3.38$ and thickness $h_1 = 0.813$ mm. The energy is first coupled from the microstrip line to the aperture. Then the cross-shaped aperture excites modes in two orthogonal directions.

When the proposed antenna is fed with a cross-shaped aperture, it can be seen that the antenna is fed by two aperture in orthogonal directions. The electric field in each of the apertures is almost constant in direction that produces a 'clean' linear polarization with low cross-pol. This means one of the aperture will only excited modes in the *x* direction and the other aperture will only excited modes in the *y* direction.

Besides, the proposed antenna has a better impedance matching than a normal patch antenna. In principle, a thin grounded substrate can be treated as a simple inductance. That will cause a narrow impedance bandwidth in normal patch antenna when the reactive part cannot be canceled. In this structure, the metasurface units on the other hand can be treated as a capacitive sheet which can be used to cancel the inductance of the grounded substrate, leading to a wide impedance bandwidth. Thus it is easy to achieve a wide impedance bandwidth by tuning the length and width of the aperture.

B. Effect of Aperture Feeding to the Axial Ratio

In the CM analysis, infinite ground plane is assumed and the feeding network is not considered. In actual design, there is a cross-shaped aperture on the ground plane. It is necessary to study the effect of the feeding on the proposed antenna.

Antenna with different size of cross-shaped apertures are studied here. The *S* parameters and the axial ratio of three different aperture size are selected and presented in Fig. 8. As is shown, the aperture size has a great influence on the *S* parameters as the conductance of the aperture change with width and length of the aperture. However, the axial ratio of the antenna does not change much. That is because the exited modes of the antenna will not change much as long as the feeding type is not changed.

There have been quite a few papers discussing the strategy of getting a good impedance matching with an aperture [4], [30], [31]. As such, details of the optimization procedure for the feeding is now presented here. The optimized parameters of the feed are listed in Table II.

C. Comparison between Full Wave Simulation and CM Theory

To better demonstrate that the proposed modes excite the circular polarization, full wave simulations is carried out with CST Microwave Studio (MWS) and the far field electric field is captured in +*z* direction. Both the amplitude and phase of the far field electric field can be obtained. The phase difference of electric field in *x* and *y* directions is calculated and compared with phase difference of different characteristic modes.

As is shown in Fig. 9, the dashed line is the phase difference of the far field electric field in *x* and *y* directions from 5 to 7 GHz. The solid line is the phase difference between mode 3 and mode 1 which are the main modes in *x* and *y* direction at lower frequencies. The dashdotted line is the phase difference between mode 7 and mode 1 which are main modes in *x* and *y*

This article has been accepted for publication in a future issue of this journal, but has not been fully edited. Content may change prior to final publication. Citation information: DOI 10.1109/ACCESS.2018.2828878, IEEE Access

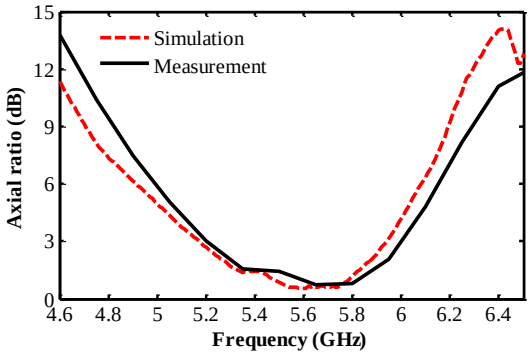

Fig. 14. Simulated and measured axial ratio at different frequencies.

directions at higher frequency between 5.7 GHz to 6 GHz. The phase difference between mode 1 and mode 3 shows a constant phase difference of around 70 degrees from 5 to 5.6 GHz which is close to 90 degrees. However, from 5.6 GHz and above, the phase difference between mode 1 and mode 3 starts to drop. Also, the main lobe of mode 3 is no longer in the +*z* direction as shown in Fig. 3. Instead, mode 7 has mode current flowing in the *x* direction and radiation pattern that radiates in the +*z* direction while mode 1 is still dominating in the *y* direction. The phase difference between mode 1 and mode 7 is also close to 90 degrees. As for far field electric field, the phase difference between the *x* and *y* directions is close to 90 degree from 5 to 6 GHz with the phase compensation from cross aperture feeding structure. That leads to a circular polarization in this frequency range.

V. Experimental Verification

The antenna is fabricated using 3 layers of substrates. The first two layers of RO4003 have a thickness of 1.524 mm to achieve an overall thickness of 3.048 mm. The patch units are printed on the top surface of the first layer of substrate. A third layer of RO4003 with the thickness of 0.813 mm is used as the feeding structure. The cross aperture is printed on the top surface while the microstrip line is printed on the bottom side. The three layers of substrates are stick together with a thin layer of nonconductive superglue. The photos of the assembly are presented in Fig. 10.

Fig. 11 depicts the simulated and measured *S* parameters. A S_{11} below −10 dB from 4.42 GHz to 6.55 GHz (38.8%) is achieved. The measured results show a good match with simulations with slight frequency shift. This difference may be attributed to the fabrication tolerance, such as additional thickness of glue and small displacement between PCBs.

The simulated and measured radiation pattern at 5.2 GHz, 5.5 GHz and 5.8 GHz is presented in Fig. 12. A good agreement between the measurement and simulation is achieved. Simulated results show a good cross polarization rejection of more than 15 dB in the boresight direction for all three frequencies. At 5.2 GHz and 5.5 GHz, there is no side lobe. But at 5.8 GHz, side lobe starts to appear because of additional modes involved. That also leads to some gain reduction at boresight. The boresight gain is shown in Fig. 13. A maximum gain of 9.4 dBic is obtained at around 5 GHz. The simulated radiation efficiency is above 90% over the operating frequency. Besides, the gain is almost constant over the operating frequency. The chamber used for measurement is typically designed for high gain antennas with a metal antenna holder. For this measurement, we have placed absorbers on the antenna holder to reduce the wave reflection from it. As such, only the front half of measured radiation pattern is presented. There is about 0.9 dB difference between the measured and simulated gain, which is quite reasonable with considering fabrication tolerance and the reflection from the antenna holder.

Fig. 14 shows the boresight axial ratio at different frequencies. As is shown, a 3 dB axial ratio bandwidth of 14.3% is obtained from 5.2 GHz to 6 GHz.

VI. Conclusion

A three step design procedure using characteristic mode theory has been used to design a wideband circular polarized patch antenna consisting of H-shaped unit cells. It has been revealed that the structure can support more than one mode in the frequency band of interest in two orthogonal directions. Cross-shaped aperture has been used to feed the antenna. With the symmetric cross-aperture feeding, only modes with symmetric current are able to be excited. These modes have a constant phase difference at a wide range of frequency, forming a wide band circular polarization. This design procedure provides great convenience for the CP antenna design by designing the radiator and feeding structure separately. That makes it much easier to design a CP antenna compared with other approaches.

A prototype of the proposed antenna has been designed and measured. The prototype has a wide impedance bandwidth of 38.8% and 3 dB axial ratio bandwidth of 14.3%. Besides, a nearly constant gain of around 8.5 dBic has been obtained over the operating frequency.

References

[1] J. R. James and P. S. Hall, *Handbook of Microstrip Antennas*, IEE Electromagnetic Waves Series, 1989.

[2] D. Pozar and D. Schaubert, *Microstrip Antennas: The Analysis and Design of Microstrip Antennas and Arrays*, New York: Jhon Wiley & Sons, Inc., 1995.

[3] T. Vlasits, "Performance of a cross-aperture coupled single feed circularly polarised patch antenna," *Electron. Lett.*, vol. 32, no. 7, pp. 612–613, 1996.

[4] S. D. Targonski and D. M. Pozar, "Design of wideband circularly polarized aperture-coupled microstrip antennas," *IEEE Trans. Antennas Propag.*, vol. 41, no. 2, pp. 214–220, 1993.

[5] H. Kim, B. M. Lee, and Y. J. Yoon, "A single-feeding circularly polarized microstrip antenna with the effect of hybrid feeding," *IEEE Antennas Wirel. Propag. Lett.*, vol. 2, no. 1, pp. 74–77, 2003.

[6] F. Yang and Y. Rahmat-Samii, "Reflection phase characterizations of the EBG ground plane for low profile wire antenna applications," *IEEE Trans. Antennas Propag.*, vol. 51, no. 10, pp. 2691–2703, Oct. 2003.

[7] H. Mosallaei and K. Sarabandi, "Antenna miniaturization and bandwidth enhancement using a reactive impedance substrate," *IEEE Trans. Antennas Propag.*, vol. 52, no. 9, pp. 2403–2414, Sep. 2004.

[8] Y. S. Chen and T. Y. Ku, "A low-profile wearable antenna using a miniature high impedance surface for smart watch applications," *IEEE Antennas Wirel. Propag. Lett.*, vol. 15, pp. 1144–1147, 2016.

[9] F. Yang and Y. Rahmat-Samii, "A low profile single dipole antenna radiating circularly polarized waves," *IEEE Trans. Antennas Propag.*, vol. 53, no. 9, pp. 3083–3086, Sep. 2005.

[10] N. Nasimuddin, Z. Chen, and X. Qing, "Bandwidth enhancement of a single-feed circularly polarized antenna using a metasurface: metamaterial-based wideband CP rectangular microstrip antenna," *IEEE Antennas Propag. Mag.*, vol. 58, no. 2, pp. 39–46, Apr. 2016.

[11] W. Liu, Z. Chen, and X. Qing, "Metamaterial-based low-profile broadband mushroom antenna," *IEEE Trans. Antennas Propag.*, vol. 62, no. 3, pp. 1165–1172, 2014.

[12] W. Liu, Z. Chen, and X. Qing, "Metamaterial-based low-profile broadband aperture-coupled grid-slotted patch antenna," *IEEE Trans. Antennas Propag.*, vol. 63, no. 7, pp. 3325–3329, 2015.

[13] R. Garbacz and R. Turpin, "A generalized expansion for radiated and scattered fields," *IEEE Trans. Antennas Propag.*, vol. 19, no. 3, pp. 348–358, 1971.

[14] R. Harrington and J. Mautz, "Theory of characteristic modes for conducting bodies," *IEEE Trans. Antennas Propag.*, vol. 19, no. 5, pp. 622–628, Sep. 1971.

[15] Y. Chen and C. F. Wang, *Characteristic Modes: Theory and Applications in Antenna Engineering*. John Wiley & Sons, Inc., 2015.

[16] B. A. Austin and K. P. Murray, "The application of characteristic-mode techniques to vehicle-mounted NVIS antennas," *IEEE Antennas Propag. Mag.*, vol. 40, no. 1, pp. 7–21, 30, 1998.

[17] E. Newman, "Small antenna location synthesis using characteristic modes," *IEEE Trans. Antennas Propag.*, vol. 27, no. 4, pp. 530–531, Jul. 1979.

[18] D. Liu, R. J. Garbacz, and D. M. Pozar, "Antenna synthesis and optimization using generalized characteristic modes," *IEEE Trans. Antennas Propag.*, vol. 38, no. 6, pp. 862–868, Jun. 1990.

[19] W. Wu and Y. P. Zhang, "Analysis of ultra-wideband printed planar quasi-monopole antennas using the theory of characteristic modes," *IEEE Antennas Propag. Mag.*, vol. 52, no. 6, pp. 67–77, Dec. 2010.

[20] J. J. Adams and J. T. Bernhard, "A modal approach to tuning and bandwidth enhancement of an electrically small antenna," *IEEE Trans. Antennas Propag.*, vol. 59, no. 4, pp. 1085–1092, Apr. 2011.

[21] Y. Chen and C. F. Wang, "Characteristic-mode-based improvement of circularly polarized U-slot and E-shaped patch antennas," *IEEE Antennas Wirel. Propag. Lett.*, vol. 11, pp. 1474–1477, 2012.

[22] Y. Chen and C. F. Wang, "Electrically small UAV antenna design using characteristic modes," *IEEE Trans. Antennas Propag.*, vol. 62, no. 2, pp. 535–545, Feb. 2014.

[23] Y. Chen and C. F. Wang, "HF band shipboard antenna design using characteristic modes," *IEEE Trans. Antennas Propag.*, vol. 63, no. 3, pp. 1004–1013, Mar. 2015.

[24] H. Li, Z. T. Miers, and B. K. Lau, "Design of orthogonal MIMO handset antennas based on characteristic mode manipulation at frequency bands below 1 GHz," *IEEE Trans. Antennas Propag.*, vol. 62, no. 5, pp. 2756–2766, May 2014.

[25] M. Khan and D. Chatterjee, "Characteristic mode analysis of a class of empirical design techniques for probe-fed, U-slot microstrip patch antennas," *IEEE Trans. Antennas Propag.*, vol. 64, no. 7, pp. 2758–2770, Jul. 2016.

[26] F. Lin and Z. Chen, "Low-profile wideband metasurface antennas using characteristic mode analysis," *IEEE Trans. Antennas Propag.*, vol. 65, no. 4, pp. 1706–1713, Apr. 2017.

[27] D. M. Pozar, "A review of aperture coupled microstrip antennas: history, operation, development, and applications," 1996. .

[28] F. Hu and C. F. Wang, "Integral equation formulations for characteristic modes of dielectric and magnetic bodies," *IEEE Trans. Antennas Propag.*, vol. 64, no. 11, pp. 4770–4776, Nov. 2016.

[29] F. Hu and C. F. Wang, "FE-BI formulations for characteristic modes," *IEEE Trans. Microw. Theory Tech.*, vol. 64, no. 5, pp. 1396–1401, May 2016.

[30] D. M. Pozar, "Microstrip antenna aperture-coupled to a microstripline," *Electron. Lett.*, vol. 21, no. 2, pp. 49–50, 1985.

[31] P. Sullivan and D. Schaubert, "Analysis of an aperture coupled microstrip antenna," *IEEE Trans. Antennas Propag.*, vol. 34, no. 8, pp. 977–984, 1986.